tvst

Article

Comparative Analysis of Multiplex Platforms for Detecting Vitreous Biomarkers in Diabetic Retinopathy

Ricardo Lamy[1,2], Suzette Farber-Katz[3], Franklin Vives[3], Gulesi Ayanoglu[3], Tong Zhao[1,2,4], Yi Chen[1,2,5], Sawarin Laotaweerungsawat[1,2,6], Dahui Ma[1,2,5], Audrey Phone[1], Catherine Psaras[1,2], Nina Xiaoyan Li[3], Santosh Sutradhar[3], Paul E. Carrington[3], and Jay M. Stewart[1,2]

[1] Department of Ophthalmology, University of California, San Francisco, San Francisco, CA, USA
[2] Department of Ophthalmology, Zuckerberg San Francisco General Hospital and Trauma Center, San Francisco, CA, USA
[3] Merck & Co., Inc., South San Francisco, CA, USA
[4] Department of Ophthalmology, China–Japan Friendship Hospital, Beijing, China
[5] Shenzhen Key Laboratory of Ophthalmology, Shenzhen Eye Hospital, Jinan University, School of Optometry, Shenzhen University, Shenzhen, China
[6] Department of Ophthalmology, Charoenkrung Pracharak Hospital, Bangkok, Thailand

Correspondence: Jay M. Stewart, University of California, San Francisco, Department of Ophthalmology, 10 Koret Way, K301, San Francisco, CA 94143-0730, USA. e-mail: jay.stewart@ucsf.edu

Received: January 14, 2020
Accepted: August 4, 2020
Published: September 2, 2020

Keywords: vitreous; cytokine, biomarker

Citation: Lamy R, Farber-Katz S, Vives F, Ayanoglu G, Zhao T, Chen Y, Laotaweerungsawat S, Ma D, Phone A, Psaras C, Li NX, Sutradhar S, Carrington PE, Stewart JM. Comparative analysis of multiplex platforms for detecting vitreous biomarkers in diabetic retinopathy. Trans Vis Sci Tech. 2020;9(10):3, https://doi.org/10.1167/tvst.9.10.3

Purpose: To evaluate the feasibility of using the Proximity Extension Assay (PEA) platform to detect biomarkers in vitreous and to compare the findings with results obtained with an electrochemiluminescent (ECL) sandwich immunoassay.

Methods: Vitreous samples from patients with proliferative diabetic retinopathy (PDR) and non-diabetic controls were tested using two different proteomics platforms. Forty-one assays were completed with the ECL platform and 459 with the PEA platform. Spearman's rank correlation coefficient (r_s) was used to determine the direction and strength of the relationship between protein levels detected by both platforms.

Results: Three hundred sixty-six PEA assays detected the tested protein in at least 25% of samples, and the difference in protein abundance between PDR and controls was statistically significant for 262 assays. Seventeen ECL assays yielded a detection rate $\geq$ 25%, and the difference in protein concentration between PDR and controls was statistically significant for 13 proteins. There was a subset of proteins that were detected by both platforms, and for those the Spearman's correlation coefficient was higher than 0.8.

Conclusions: PEA is suitable for the analysis of vitreous samples, showing a strong correlation with the ECL platform. The detection rate of PEA panels was higher than the panels tested with ECL. The levels of several proinflammatory and angiogenic cytokines were significantly higher in PDR vitreous compared to controls.

Translational Relevance: This study provides new information on the yields of small-volume assays that can detect proteins of interest in ocular specimens, and it identifies patterns of cytokine dysregulation in PDR.

Introduction

Vitreous is a gel matrix consisting mainly of water, collagen, and hyaluronan that fills approximately 80% of the eye structure and is surrounded by the retina, ciliary body, and lens.[1–3] The levels of proinflammatory cytokines and proteins are increased in the vitreous in a number of uveal and retinal disorders, and that can play a role in the pathogenesis of many retinal diseases, including proliferative diabetic retinopathy (PDR).[4–8]

The proximity of human vitreous to the retina makes it a useful source of biomarkers for retinal conditions, but research has been limited by the difficulty in obtaining and processing adequate volumes of vitreous samples. Traditional singleplex enzyme-

Copyright 2020 The Authors

This work is licensed under a Creative Commons Attribution-NonCommercial-NoDerivatives 4.0 International License.

Downloaded from abstracts.iovs.org on 04/19/2024

linked immunosorbent assays (ELISAs) measure a colored or fluorescent product generated by enzymes employed to show antigen–antibody reactions and can be very accurate, such that characterization of a single analyte is sufficient, but they are impractical for biomarker screening.[9,10] More recently, novel multiplexing technologies have been developed for the detection of several proteins in small volumes of biospecimens.[11–13] Multiplexing techniques are commonly used to detect biomarkers in serum and plasma.[14] Interactions between different biofluid matrices and multiplexed analytical methods can interfere with the detection rates of many cytokines[15,16]; thus, it is important to know how these new technologies perform on other biofluids such as the vitreous.

We have previously reported the successful use of an electrochemiluminescent (ECL) sandwich immunoassay (Meso Scale Discovery, MSD) to detect potential biomarkers in the human vitreous.[17] More recently, a new platform based on Proximity Extension Assay (PEA) has been demonstrated to be a useful resource for biomarker screening and target discovery, allowing a higher level of multiplexing for the detection of hundreds of proteins of interest using minute volumes of biofluids.[18–20] The purpose of this study was to evaluate for the first time, to the best of our knowledge, the feasibility of using PEA on vitreous gel samples from patients with and without diabetic retinopathy and to compare the findings with the results obtained with an ECL sandwich immunoassay.

Methods

This study was approved by the Human Research Protection Program at the University of California, San Francisco (UCSF) and adhered to the tenets of the Declaration of Helsinki. Twenty diabetic patients with PDR and 17 nondiabetic controls undergoing primary pars plana vitrectomy at UCSF Medical Center and Zuckerberg San Francisco General Hospital and Trauma Center from October 2016 to June 2018 were recruited. Patients were ineligible if they had a history of prior vitrectomy, rhegmatogenous retinal detachment, retinal vascular occlusion, uveitis, advanced glaucoma, complicated anterior segment surgery, or trauma. Clinical characteristics were collected from the medical record, including history of cataract surgery, recent intravitreal injection of anti-vascular endothelial growth factor (VEGF) agents (within the last 90 days), and prior panretinal photocoagulation.

Vitreous samples were collected during vitrectomy surgery. Before fluid infusion was turned on, a undiluted sample of vitreous was obtained with the vitreous cutter using 25- or 27-gauge vitrectomy. All samples were immediately flash frozen and stored at –80°C. ECL sandwich multiplex immunoassay was performed on vitreous samples according to the manufacturer's protocol using the MSD V-PLEX Human Biomarker Kit (Meso Scale Discovery, Rockville, MD) consisting of five multiplex panels: proinflammatory, cytokine, chemokine, angiogenesis, and vascular injury. All of the assays in the panels are calibrated against a reference calibrator, and the concentration results are given in pg/mL. For the purpose of statistical analyses, as a conservative approach the zero values were treated as the value of the minimum reportable concentration (MRC). The PEA was performed on vitreous samples by Olink Proteomics (Uppsala, Sweden) using the Human Olink Platform, consisting of five panels: cardiometabolic, cell regulation, development, immuno-oncology, and inflammation. Raw values were normalized for variation using internal and external controls and were converted into normalized protein expression units (NPX), which are arbitrary units on a logarithmic scale, allowing for the relative quantification of proteins. For correlation against ECL values, which are linear, the PEA NPX values, which are in a $\log_2$ format, were linearized according to the manufacturer's instructions using the equation 2^{NPX} = linear NPX.

Prism 8.3 (GraphPad Software, San Diego, CA) and the MULTTEST procedure in SAS 9.4 (SAS Institute, Cary, NC) were used to perform statistical analyses and plot correlation graphs. The difference in sex distribution and lens status was calculated with Fisher's exact test. The difference in age was compared with Student's *t*-test. The Spearman's rank correlation coefficient (r_s) was used to determine the direction and the strength of the relationship between platforms for proteins that were detected in at least 70% of the samples by both platforms. In order to test whether the correlation was statistically significant for each protein, a *P* value for testing correlation coefficient > 0 was calculated based on a *t*-distribution. For each platform (ECL or PEA) and each protein, the mean difference (PDR vs. control) was compared using two-sample *t*-tests assuming unequal variance between the comparison groups. Due to skewness in the ECL values, natural log transformation was used before the analysis and, for PEA, NPX values were used for the comparative analysis. For certain proteins, mostly in the control group, all values were at MRCs, reflecting zero variability within the group. The proteins with all values at the MRC were excluded from analysis. Due to the large number of proteins assessed, *P* values controlled by the false discovery rate (FDR-*P*) were calculated by adjusting

Downloaded from abstracts.iovs.org on 04/19/2024

Table 1. Patient Characteristics

	PDR ($n = 20$)	Control ($n = 17$)	P
Age, y			<0.0001[a]
Mean ± SD (range)	50.56 ± 10.08 (26–77)	65.77 ± 7.50 (53–78)	
Median (IQR)	51.27 (46.6–55.5)	64.42 (59.5–71.6)	
Sex, *n*			0.008[b]
Female	4	11	
Male	16	6	
Lens status, *n*			0.069[b]
Phakic	17	9	
Pseudophakic	3	8	
Indication for vitrectomy, *n*			N/A
ERM	—	8	
Macular hole	—	4	
VMA	—	1	
Vitreous floaters	—	4	
VH	9	—	
TRD	7	—	
TRD + VH	3	—	
NVI	1	—	
Hemoglobin A1c, %			N/A
Mean ± SD (range)	8.2 ± 2.2 (5.4–12)	—	
Median (IQR)	8.0 (6.1–10)	—	
Recent intravitreal injection (within 90 days), *n*	8[c]	—	—
History of PRP, *n*	11	—	—

SD, standard deviation; IQR, interquartile range; ERM, epiretinal membrane; VMA, vitreomacular adhesion; VH, vitreous hemorrhage; TRD, traction retinal detachment; NVI, neovascularization of the iris; PRP, panretinal photocoagulation.

[a]Student's *t*-test.

[b]Fisher's exact test.

[c]Recent intravitreal injections included anti-VEGF medications in seven eyes and triamcinolone acetonide in one eye.

P values using the linear step-up method of Benjamini and Hochberg.[21] A statistically significant difference in the level of a protein was defined by a FDR-$P < 0.05$. The resulted mean difference (PDR vs. control), its 95% confidence interval, and the corresponding FDR-*P* values were calculated.

Results

Vitreous samples were collected from diabetic PDR patients ($n = 20$) and nondiabetic controls ($n = 17$) (Table 1). All subjects were able to provide a sufficient volume of specimen for analysis. Vitreous was analyzed using assays from the ECL and PEA platforms. Each assay measures one protein. A total of 41 assays from five panels were completed with the ECL platform, and 459 assays from five panels were completed with the PEA platform. Due to panel overlap, some proteins were detected by more than one panel within the same platform; for example, IL-8 was tested by two PEA panels (inflammation and immuno-oncology) and two ECL panels (proinflammatory and chemokine). The sensitivity and dynamic range of detection of each cytokine may vary depending on the main purpose of each commercially available panel; therefore, the results of each panel were presented separately and analyzed as independent variables (Table 2).

Using the PEA platform, 93 protein assays yielded a detection rate lower than 25%, meaning that for those 93 proteins more than 75% of the tested samples yielded undetectable values. Thus, the other 366 assays yielded detectable results in at least 25% of the samples. The difference between PDR and non-diabetics was statistically significant for 262 assays (Supplementary Table S1) based on FDR-controlled *P* values at the 5% level. The vast majority of those proteins (259) were elevated in PDR samples relative to non-diabetic

Downloaded from abstracts.iovs.org on 04/19/2024

Table 2. Detection Rate for Proteins Identified in Human Vitreous Specimens Using ECL and PEA Platforms

	ECL			PEA		
		Detection (%)			Detection (%)	
Protein	Panel	Control	PDR	Panel	Control	PDR
Eotaxin	CH	0.0	0.0	IN	100.0	100.0
FGF2	AN	20.0	7.1	IO	23.5	5.0
ICAM-1	VI	100.0	100.0	CM	70.6	100.0
IFN-γ	PI	0.0	0.0	IO	11.8	5.0
				IN	0.0	0.0
IL-1α	CY	11.8	25.0	IO	0.0	0.0
				IN	0.0	0.0
IL-2	PI	0.0	5.0	IO	0.0	10.0
				IN	0.0	0.0
IL-4	PI	0.0	5.0	IO	17.6	15.0
				IN	5.9	5.0
IL-5	CY	0.0	0.0	IO	0.0	0.0
				IN	0.0	0.0
IL-6	PI	94.1	100.0	IO	100.0	100.0
				IN	100.0	100.0
IL-7	CY	100.0	100.0	IO	100.0	100.0
				IN	100.0	100.0
IL8	CH	0.0	5.3	IO	100.0	100.0
	PI	100.0	100.0	IN	100.0	100.0
IL-10	PI	0.0	5.0	IO	11.8	5.0
				IN	0.0	25.0
IL-12p40	CY	94.1	100.0	IN	100.0	100.0
IL-12p70	PI	0.0	0.0	IO	100.0	100.0
IL-13	PI	0.0	0.0	IO	5.9	5.0
				IN	5.9	5.0
IL-17A	CY	0.0	0.0	IN	17.6	25.0
IP-10	CH	100.0	100.0	IO	100.0	100.0
				IN	100.0	100.0
MCP-1	CH	100.0	100.0	IO	100.0	100.0
				IN	100.0	100.0
MCP-4	CH	0.0	10.5	IO	100.0	100.0
				IN	5.9	45.0
MIP-1α	CH	0.0	10.5	IO	100.0	100.0
				IN	100.0	100.0
MIP-1β	CH	100.0	100.0	IO	100.0	100.0
				IN	100.0	100.0
PGF	AN	0.0	100.0	IO	100.0	100.0
TARC	CH	0.0	42.1	IO	100.0	100.0
Tie-2	AN	0.0	0.0	IO	100.0	100.0
TNF-α	PI	0.0	30.0	IO	0.0	0.0
				IN	5.9	5.0
TNF-β	CY	0.0	5.0	IN	76.5	95.0
VCAM-1	VI	70.6	94.7	CM	23.5	50.0
	AN	26.7	100.0	IO	100.0	100.0
VEGF-A	CY	6.3	90.0	IN	100.0	100.0
VEGF-C	AN	6.7	7.1	IO	94.1	95.0
VEGF-D	AN	0.0	35.7	CR	88.2	100.0

FGF2, fibroblast growth factor 2; ICAM-1, intercellular adhesion molecule 1; IFN-γ, interferon gamma; IL-1α, interleukin 1 alpha; IP-10, IFN-γ-induced protein 10; MCP-1, monocyte chemoattractant protein-1; MIP-1α, macrophage inflammatory protein 1 alpha; PGF, placental growth factor; TARC, thymus and activation-regulated chemokine; Tie2, tyrosine kinase receptor; TNF-α, tumor necrosis factor alpha; VCAM-1, vascular cell adhesion molecule 1; VEGF-A, vascular endothelial growth factor A. Panels: CH, chemokine (control, $n = 17$; diabetic, $n = 19$); AN, angiogenesis (control, $n = 15$; diabetic, $n = 14$); VI, vascular injury (control, $n = 17$; diabetic, $n = 19$); PI, proinflammatory (control, $n = 17$; diabetic, $n = 20$); CY, cytokine (control, $n = 17$; diabetic, $n = 20$); IN, inflammation (control, $n = 17$; diabetic, $n = 20$); IO, immuno-oncology (control, $n = 17$; diabetic, $n = 20$); CM, cardiometabolic (control, $n = 17$; diabetic, $n = 20$); CR, cell regulation (control, $n = 17$; diabetic, $n = 19$).

control samples. Only three proteins were significantly more abundant in control samples (interleukin 13 receptor, arylsulfatase B, and pleiotrophin).

Figure 1 provides a forest plot of the mean differences between the PDR and control groups for the top proteins tested with the PEA platform, ranked by magnitude of difference. For all proteins with FDR-$P < 0.05$, data are presented in Supplementary Table S1. Seventeen ECL assays yielded a detection rate equal or greater than 25%, and 24 assays yielded a detection rate lower than 25%. The difference between the PDR and non-diabetic groups was statistically significant for 13 proteins (all elevated in PDR samples) based on FDR-controlled P values at the 5% level. A forest plot of the statistically significant results from the ECL platform is presented in Figure 2.

Thirty proteins were measured by both platforms. The detection rates of those analytes and the number of vitreous samples that passed on quality control in each panel are presented in Table 2.

Spearman's correlation scatterplots are presented for the proteins that were detected by both technologies in at least 70% of the samples (Fig. 3).

translational vision science & technology

Downloaded from abstracts.iovs.org on 04/19/2024

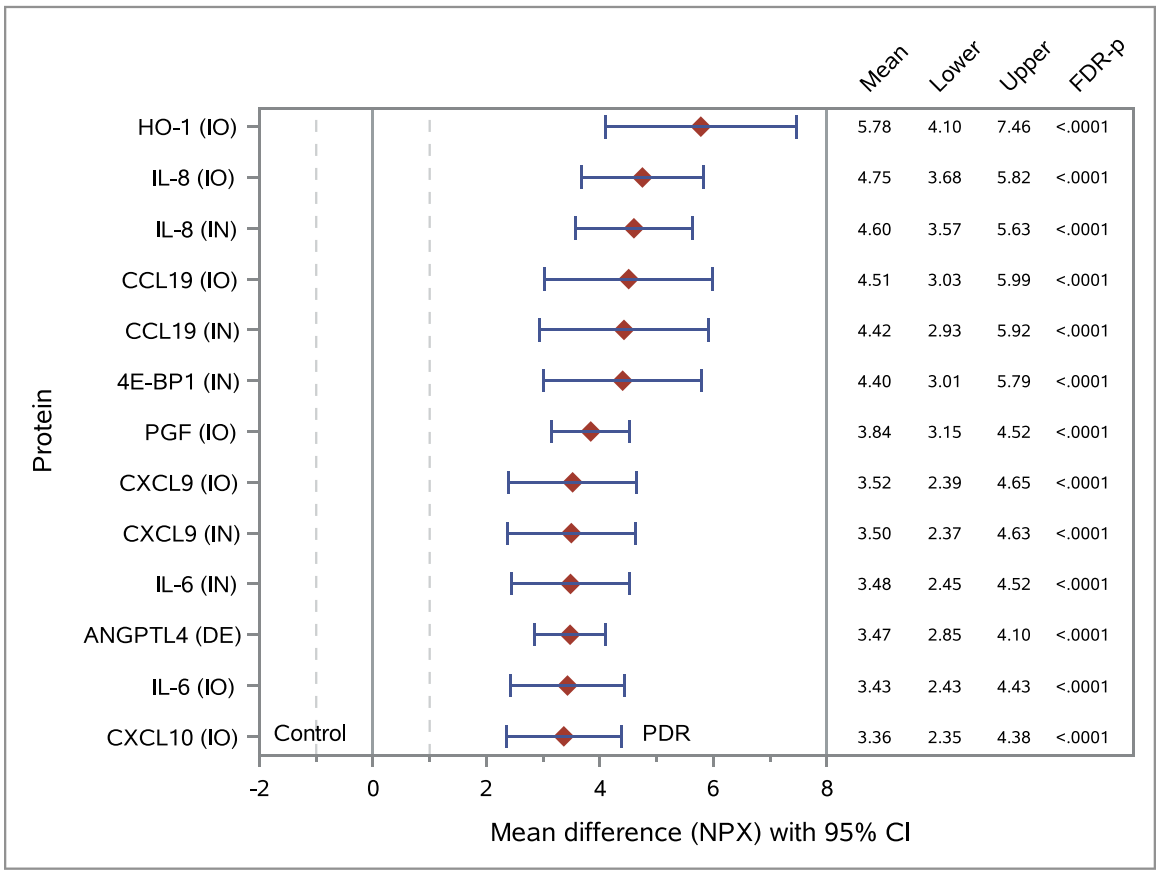

Figure 1. Forest plot of mean difference between the PDR and control groups and corresponding 95% confidence intervals (CIs) for proteins identified in vitreous specimens using the PEA platform. Protein levels are measured in NPX units. Results are ranked by magnitude of difference for selected top 13 proteins with FDR-$P < 0.05$. Unequal variance by group (PDR vs. control) was used for calculating the *t*-test statistic. Assay panels: IO, immuno-oncology (control, $n = 17$; PDR, $n = 20$); IN, inflammation (control, $n = 17$; PDR, $n = 20$); DE, development (control, $n = 17$; PDR, $n = 20$). Protein levels were higher in the vitreous of diabetic patients with proliferative diabetic retinopathy when compared to non-diabetic controls, suggesting potential vitreous biomarkers for diabetic retinopathy.

Discussion

In the present study, we show for the first time, to the best of our knowledge, the ability of PEA to detect the abundance of several proteins in human vitreous and how the results correlate with those of ECL multiplex assays. We also show what proteins were adequately detected, and we present the top significant discoveries when comparing the vitreous of PDR and control patients in each of the platforms.

Vascular endothelial growth factor was one of the first diffusible angiogenic proteins to be detected at high levels in the vitreous of eyes with ischemic retinas and to be identified as a contributor to neovascularization of the retina, optic nerve, and iris.[22] It became a crucial therapeutic target, and, since 2004, intravitreal injections of anti-VEGF drugs have become a very common clinic-based treatment for a variety of exudative retinal diseases.[23] Although anti-VEGF drugs were a major breakthrough in the treatment of exudative retinal diseases, there is a great need to find new therapeutic targets because some patients exhibit a poor response or experience a loss of efficacy after repeated administration of anti-VEGF agents over time.[24]

When searching for new biological markers and drug targets in biological fluids, multiplexed immunoassays are often preferred over single-analyte ELISAs because they allow the screening of several proteins at once in a small volume of biological fluid. The ECL sandwich immunoassay platform uses plate-based capture antibodies, coated on up to 10 independent spots per well, allowing for multiplexing of up to 10 protein targets per panel (Fig. 4). Instead of detecting colorimetric substrates, which are common in ELISAs, the ECL platform uses secondary detec-

Downloaded from abstracts.iovs.org on 04/19/2024

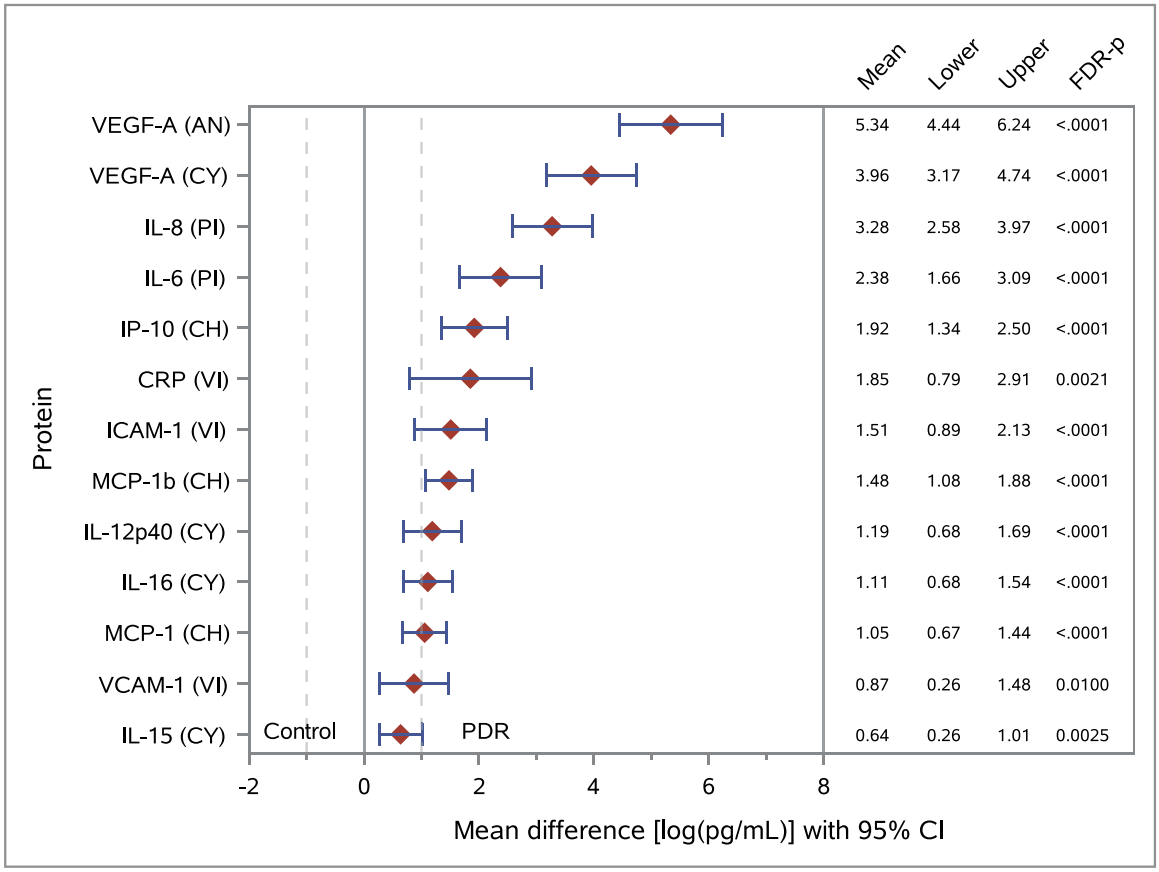

Figure 2. Forest plot of mean differences between the PDR and control groups and corresponding 95% CIs for proteins identified in vitreous specimens using the ECL platform. Results are ranked by magnitude of difference for selected proteins with FDR-$P < 0.05$. Natural log-transformed values of protein levels are in pg/mL. Unequal variance by group (PDR vs. control) was used for calculating the *t*-test statistic. Assay panels: PI, proinflammatory (control, $n = 17$; PDR, $n = 20$); CY, cytokine (control, $n = 17$; PDR, $n = 20$); CH, chemokine (control, $n = 17$; PDR, $n = 19$); VI, vascular injury (control, $n = 17$; PDR, $n = 19$). Protein levels were higher in the vitreous of diabetic patients with proliferative diabetic retinopathy when compared to non-diabetic controls, suggesting potential vitreous biomarkers for diabetic retinopathy.

tion antibodies conjugated to electrochemiluminescent labels that emit light when electricity is applied to the working electrodes. By not relying on colorimetric substrates, the ECL platform has improved reproducibility, and the application of multiple electrical excitation cycles amplifies the light intensity for lower protein levels, increasing the sensitivity of the assay.[25] Each panel uses 25 µL of sample per replicate and yields absolute values of protein content in pg/mL.

Compared to the ECL platform, the PEA platform offers the advantage of measuring many more proteins, up to 92 per panel, using a very low volume of sample (1 µL). Instead of using one capture and one electrochemiluminescent-labeled detection antibody, the PEA technology utilizes a pair of antibodies conjugated to complementary sequences of DNA oligonucleotides, also known as proximity probes (Fig. 4). The antibodies target epitopes on the same protein of interest, and after binding to their respective targets the attached probes are brought into proximity and hybridize. The oligonucleotides are then extended by a DNA polymerase and form a unique polymerase (PCR) amplicon that can be quantified using quantitative real-time PCR (qPCR). The PCR-based amplification step is the key step that allows the method to utilize an exceptionally low volume of sample for each panel. Another main advantage is that the proximity probes only anneal if both antibodies are bound to the same protein; thus, cross-reactive antibody events are unlikely to lead to amplification, which should reduce the occurrence of false positives. PEA has been successfully used to detect plasma biomarkers for cancer and cardiovascular diseases.[26–28]

According to both manufacturers, more than 80% of the assays are expected to detect proteins on ethylenediaminetetraacetic acid-treated plasma from healthy donors. In our study, using the PEA platform, 79.7% of the assays were able to detect proteins in at

Downloaded from abstracts.iovs.org on 04/19/2024

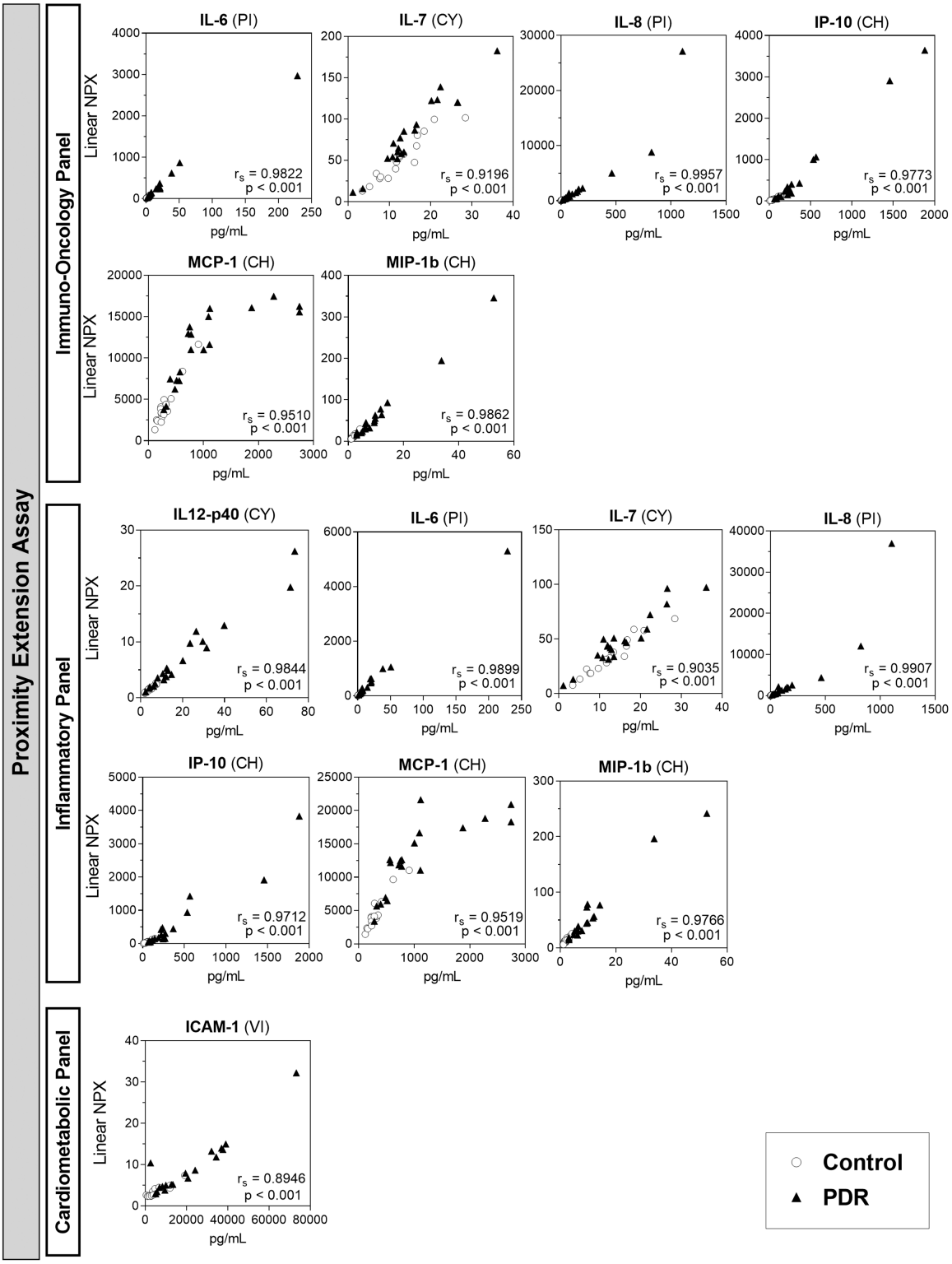

Figure 3. Scatterplot of Spearman's correlation between PEA and ECL platforms for proteins detected in at least 70% of specimens. *Y*-axis: protein levels measured with the PEA platform, in linear normalized protein expression (NPX) units; *X*-axis: protein levels measured with the ECL platform, in pg/mL. ECL assay panels in parentheses: PI, proinflammatory (control, $n = 17$; PDR, $n = 20$); CY, cytokine (control, $n = 17$; PDR, $n = 20$); CH, chemokine (control, $n = 17$; PDR, $n = 19$); VI, vascular injury (control, $n = 17$; PDR, $n = 19$). Controls (*open circles*) and PDR (*closed triangles*). Regardless of the platform panel, there is a strong correlation (Spearman's coefficient $r_s > 0.8$, $P < 0.001$) between protein levels detected by assays from both platforms.

Downloaded from abstracts.iovs.org on 04/19/2024

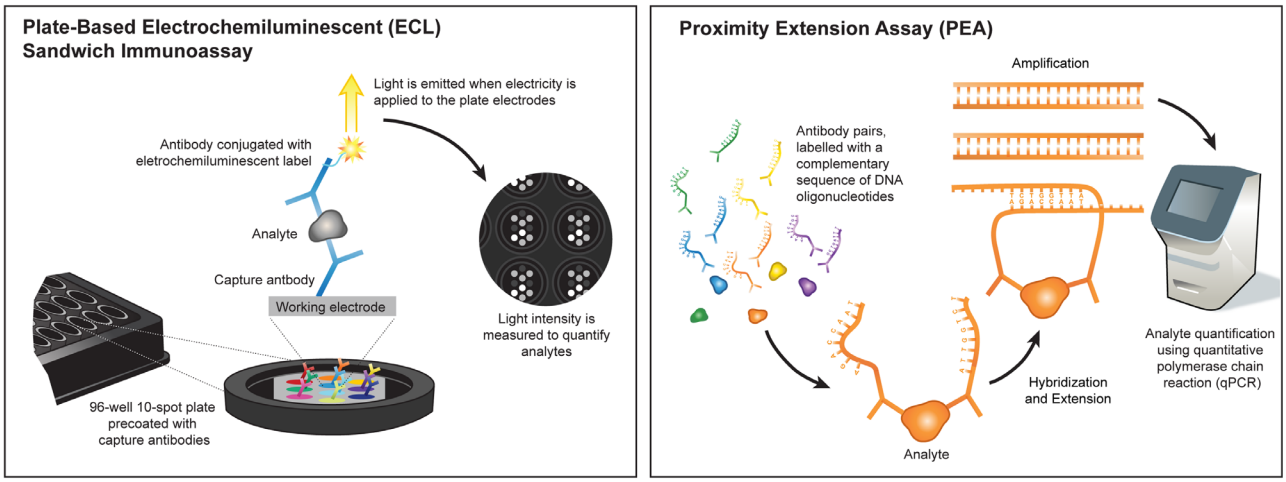

Figure 4. Illustration of assay mechanisms for the ECL and PEA platforms. ECL is a plate-based technology, and currently up to 10 proteins can be measure per panel. The PEA platform uses qPCR technology to detect protein abundance levels and can measure up to 92 proteins per panel.

least 25% of the vitreous samples, whereas only 41.5% of the ECL assays detected proteins in more than 25% of the vitreous samples. These lower detectability rates compared to those reported for plasma may have resulted from differences in protein abundance between plasma and vitreous and the non-specific background. Also, interactions between the matrix and multiplexed analytical methods can interfere with the detection rates of many cytokines.[15,29] The amplification step and qPCR-based detection method incorporated in the PEA platform may explain the higher detection rates in vitreous samples with low protein abundance when compared to the ECL platform. Out of the 30 proteins measured by both platforms, the ECL assays showed a better detection rate for interleukin 1 alpha (IL-1α), tumor necrosis factor alpha (TNF-α), intercellular adhesion molecule 1 (ICAM-1), and vascular cell adhesion molecule 1 (VCAM-1). In contrast, the PEA assays showed a better detection rate for eotaxin, fibroblast growth factor 2 (FGF2), interferon gamma (IFN-γ), IL-2, IL-4, IL-6, IL-10, IL-12p40, IL-12p70, IL-13, IL-17α, monocyte chemoattractant protein-4 (MCP-4), macrophage inflammatory protein 1 alpha (MIP-1α), placental growth factor (PGF), thymus and activation-regulated chemokine (TARC), tyrosine kinase receptor (Tie2), tumor necrosis factor beta (TNF-β), VEGF-A, VEGF-C, and VEGF-D. Neither platform detected IL-5 in the vitreous samples.

Analytes that have a very high abundance in human plasma, such as C-reactive protein (CRP), are not currently offered on PEA panels, possibly because they would require further dilution, making it difficult to multiplex with other less abundant analytes using PEA technology. CRP is present on the ECL vascular injury panel, and it was detected in 86.1% of the vitreous samples. Other PEA limitations include the arbitrary unit and relative quantification of proteins normalized to internal and external controls. Also, differences in data processing can affect intersite replicability and lead to inconsistencies among reported findings.[25]

For proteins that were well detected by both platforms, our results show a strong correlation between protein levels in the respective assays. The correlation was strong (r_s higher than 0.8) even when analyzing only samples from the PDR group separately (data not shown). This finding suggests that, despite the difference in the unit of measurement, the results of both platforms can be compared when studying the vitreous of control and diabetic populations by using rank values.

In our study, when comparing PDR with controls, we found several proteins that showed a statistically significant difference, and we used the Benjamini–Hochberg FDR correction to limit false discoveries.[21,30] Breakdown of the blood–retinal barrier is common in diabetic retinopathy, and vitreous hemorrhage was present in some samples of the PDR group. Both alterations may explain the overall higher levels of proteins detected in the vitreous of the PDR group.[31–34] One of the top proteins on the PEA discovery list is PGF, a well-studied angiogenic growth factor and homolog of VEGF. Recently, Kahtani and colleagues[35] reported a strong correlation for PGF levels with PDR status, with significantly higher levels of PGF being detected in the vitreous of patients with active PDR.

VEGF-A presented the highest magnitude of difference between control and PDR samples with the ECL

Downloaded from abstracts.iovs.org on 04/19/2024

platform. That difference was likely muted because, within the PDR group, 35% of the patients ($n = 7$) had received an intravitreal injection of anti-VEGF therapy (bevacizumab) within the 3 months preceding the vitreous collection. Bevacizumab is a humanized monoclonal antibody that binds to all isoforms of VEGF-A. The half-life of bevacizumab in animal model eyes is 4.32 days, but it has been reported that concentrations of >10 µg/mL bevacizumab can be maintained in the vitreous humor for 30 days.[36]

Monocyte chemoattractant protein-1 (MCP-1) is one of the proteins with significant difference detected by our ECL and PEA assays. It is a proinflammatory cytokine known for recruiting monocytes and macrophages. Through their research studying the vitreous concentration of four cytokines (MCP-1, IL-6, IL-8, and VEGF) using a cytometric bead array, Yoshida and colleagues[37] suggested that high levels of MCP-1 can be an important contributing factor to postoperative diabetic macular edema in vitrectomized eyes.

IL-8 was present in the top three ranks of both ECL and PEA forest plots. Higher levels of IL-8 were detected in vitreous from diabetic patients compared to control. IL-8 is a proinflammatory cytokine released from retinal endothelial and glial cells in response to hypoxia and is involved in inflammation-mediated angiogenesis. High levels of IL-8 have been previously reported in the vitreous of diabetic patients and have been related to subretinal fluid formation and poor visual outcome after vitrectomy.[38,39]

This study has some limitations with regard to comparing the diabetic and non-diabetic control samples, as they were not perfectly matched for age and sex. Vitreous structure changes with aging. There is an increase in liquefaction and fiber aggregation, and the vitreous protein content may vary reflecting underlying vitreoretinal diseases that are more common in older age.[40–44]

The presence and severity of PDR are more associated with male sex,[45] and the mean age of the controls was greater than that of diabetic PDR patients, because the indications for vitrectomy in controls predominantly affect older patients. Further studies may use PEA to investigate the proteomic composition of the vitreous among groups of patients with diabetic retinopathy at different stages and compared to age- and sex-matched controls.

In summary, our results suggest that the PEA platform is suitable for the analysis of vitreous samples, and it showed a strong correlation with the ECL platform for proteins that were well detected by both platforms. The detection rate of the tested PEA panels was higher than the panels tested with the ECL platform for vitreous samples from the diabetic and control groups. The levels of several proinflammatory and angiogenic cytokines were significantly higher in the vitreous of diabetic patients compared to controls.

Acknowledgments

The authors thank the assistance of Suling Wang in preparing the illustration of assay mechanisms (Fig. 4).

Supported in part by the National Institutes of Health National Eye Institute (Core Grant for Vision Research EY002162 and 1R01EY024004 to J.M.S.); Research to Prevent Blindness; That Man May See; and Merck Sharp & Dohme Corp., a subsidiary of Merck & Co., Inc.

Disclosure: **R. Lamy**, None; **S. Farber-Katz**, None; **F. Vives**, None; **G. Ayanoglu**, None; **T. Zhao**, None; **Y. Chen**, None; **S. Laotaweerungsawat**, None; **D. Ma**, None; **A. Phone**, None; **C. Psaras**, None; **N.X. Li**, None; **S. Sutradhar**, None; **P.E. Carrington**, None; **J.M. Stewart**, None

References

1. Bishop PN. Structural macromolecules and supramolecular organisation of the vitreous gel. *Prog Retin Eye Res*. 2000;19:323–344.
2. de Smet MD, Gad Elkareem AM, Zwinderman AH. The vitreous, the retinal interface in ocular health and disease. *Ophthalmologica*. 2013;230:165–178.
3. Sebag J. *The Vitreous: Structure, Function, and Pathobiology*. New York, NY: Springer-Verlag; 2012:35–58.
4. Dai Y, Wu Z, Wang F, Zhang Z, Yu M. Identification of chemokines and growth factors in proliferative diabetic retinopathy vitreous. *Biomed Research Int*. 2014;2014:486386.
5. Takeuchi M, Sato T, Tanaka A, et al. Elevated levels of cytokines associated with Th2 and Th17 cells in vitreous fluid of proliferative diabetic retinopathy patients. *PLoS One*. 2015;10:e0137358.
6. Agrawal R, Iyer J, Connolly J, Iwata D, Teoh S. Cytokines and biologics in non-infectious autoimmune uveitis: bench to bedside. *Indian J Ophthalmol*. 2014;62:74–81.
7. Rübsam A, Parikh S, Fort PE. Role of inflammation in diabetic retinopathy. *Int J Mol Sci*. 2018;19:942.

Downloaded from abstracts.iovs.org on 04/19/2024

8. Banerjee S, Savant V, Scott RAH, Curnow SJ, Wallace GR, Murray PI. Multiplex bead analysis of vitreous humor of patients with vitreoretinal disorders. *Invest Ophthalmol Vis Sci*. 2007;48:2203–2207.
9. Tighe PJ, Ryder RR, Todd I, Fairclough LC. ELISA in the multiplex era: potentials and pitfalls. *Proteomics Clin Appl*. 2015;9:406–422.
10. Aydin S. A short history, principles, and types of ELISA, and our laboratory experience with peptide/protein analyses using ELISA. *Peptides*. 2015;72:4–15.
11. Chen J, Schwarz E. Opportunities and challenges of multiplex assays: a machine learning perspective. *Methods Mol Biol*. 2017;1546:115–122.
12. Chen J, Guest PC, Schwarz E. The utility of multiplex assays for identification of proteomic signatures in psychiatry. *Adv Exp Med Biol*. 2017;974:131–138.
13. Adamcova M, Šimko F. Multiplex biomarker approach to cardiovascular diseases. *Acta Pharmacol Sin*. 2018;39:1068–1072.
14. Rosenberg-Hasson Y, Hansmann L, Liedtke M, Herschmann I, Maecker HT. Effects of serum and plasma matrices on multiplex immunoassays. *Immunol Res*. 2014;58:224–233.
15. Hoadley ME, Hopkins SJ. Overcoming matrix matching problems in multiplex cytokine assays. *J Immunol Methods*. 2013;396:157–162.
16. Rosenberg-Hasson Y, Hansmann L, Liedtke M, Herschmann I, Maecker H. Effects of serum and plasma matrices on multiplex immunoassays. *Immunol Res*. 2014;58:224–233.
17. Wu F, Phone A, Lamy R, et al. Correlation of aqueous, vitreous, and plasma cytokine levels in patients with proliferative diabetic retinopathy. *Invest Ophthalmol Vis Sci*. 2019;61:26.
18. Assarsson E, Lundberg M, Holmquist G, et al. Homogenous 96-Plex PEA immunoassay exhibiting high sensitivity, specificity, and excellent scalability. *PLoS One*. 2014;9:e95192.
19. Thorsen SB, Lundberg M, Villablanca A, et al. Detection of serological biomarkers by proximity extension assay for detection of colorectal neoplasias in symptomatic individuals. *J Transl Med*. 2013;11:253.
20. Lind L, Siegbahn A, Lindahl B, Stenemo M, Sundström J, Ärnlöv J. Discovery of new risk markers for ischemic stroke using a novel targeted proteomics chip. *Stroke*. 2015;46:3340–3347.
21. Benjamini Y, Hochberg Y. Controlling the false discovery rate: a practical and powerful approach to multiple testing. *J R Stat Soc Ser B Methodol*. 1995;57:289–300.
22. Miller JW, PA Anthony, David TS, et al. Vascular endothelial growth factor/vascular permeability factor is temporally and spatially correlated with ocular angiogenesis in a primate model. *Am J Pathol*. 1994;145:574–584.
23. Kim LA, D'Amore PA. A brief history of anti-VEGF for the treatment of ocular angiogenesis. *Am J Pathol*. 2012;181:376–379.
24. Yang S, Zhao J, Sun X. Resistance to anti-VEGF therapy in neovascular age-related macular degeneration: a comprehensive review. *Drug Des Devel Ther*. 2016;10:1857–1867.
25. Carlyle BC, Trombetta BA, Arnold SE. Proteomic approaches for the discovery of biofluid biomarkers of neurodegenerative dementias. *Proteomes*. 2018;6:32.
26. Alhamdow A, Lindh C, Albin M, Gustavsson P, Tinnerberg H, Broberg K. Cardiovascular disease-related serum proteins in workers occupationally exposed to polycyclic aromatic hydrocarbons. *Toxicol Sci*. 2019;171:235–246.
27. Alhamdow A, Tinnerberg H, Lindh C, Albin M, Broberg K. Cancer-related proteins in serum are altered in workers occupationally exposed to polycyclic aromatic hydrocarbons: a cross-sectional study. *Carcinogenesis*. 2019;40:771–781.
28. Berggrund M, Enroth S, Lundberg M, et al. Identification of candidate plasma protein biomarkers for cervical cancer using the multiplex proximity extension assay. *Mol Cell Proteomics*. 2019;18:735–743.
29. Rosenberg-Hasson Y, Hansmann L, Liedtke M, Herschmann I, Maecker HT. Effects of serum and plasma matrices on multiplex immunoassays. *Immunol Res*. 2014;58:224–233.
30. Karp NA, McCormick PS, Russell MR, Lilley KS. Experimental and statistical considerations to avoid false conclusions in proteomics studies using differential in-gel electrophoresis. *Mol Cell Proteomics*. 2007;6:1354–1364.
31. Cunha-Vaz J. Blood-retinal barrier and its relevance in retinal disease. *Med Retina*. 2012;1:6–10.
32. Palenski TL, Sorenson CM, Sheibani N. Inflammatory cytokine-specific alterations in retinal endothelial cell function. *Microvasc Res*. 2013;89:57–69.
33. Elner SG, Elner VM, Jaffe GJ, Stuart A, Kunkel SL, Strieter RM. Cytokines in proliferative diabetic retinopathy and proliferative vitreoretinopathy. *Curr Eye Res*. 1995;14:1045–1053.
34. Asrar AE, Ahmed M, Maimone D, Morse PH, Gregory S, Reder AT. Cytokines in the vitreous of

Downloaded from abstracts.iovs.org on 04/19/2024

patients with proliferative diabetic retinopathy. *Am J Ophthalmol*. 1992;114:731–736.
35. Al Kahtani E, Xu Z, Al Rashaed S, et al. Vitreous levels of placental growth factor correlate with activity of proliferative diabetic retinopathy and are not influenced by bevacizumab treatment. *Eye (Lond)*. 2017;31:529–536.
36. Bakri SJ, Snyder MR, Reid JM, Pulido JS, Singh RJ. Pharmacokinetics of intravitreal bevacizumab (Avastin). *Ophthalmology*. 2007;114:855–859.
37. Yoshida S, Kubo Y, Kobayashi Y, et al. Increased vitreous concentrations of MCP-1 and IL-6 after vitrectomy in patients with proliferative diabetic retinopathy: possible association with postoperative macular oedema. *Br J Ophthalmol*. 2015;99:960–966.
38. Yenihayat F, Özkan B, Kasap M, et al. Vitreous IL-8 and VEGF levels in diabetic macular edema with or without subretinal fluid. *Int Ophthalmol*. 2019;39:821–828.
39. Koskela UE, Kuusisto SM, Nissinen AE, Savolainen MJ, Liinamaa MJ. High vitreous concentration of IL-6 and IL-8, but not of adhesion molecules in relation to plasma concentrations in proliferative diabetic retinopathy. *Ophthalmic Res*. 2013;49:108–114.
40. Sebag J. Ageing of the vitreous. *Eye*. 1987;1:254–262.
41. Lumi X, Hawlina M, Glavač D, et al. Ageing of the vitreous: from acute onset floaters and flashes to retinal detachment. *Ageing Res Rev*. 2015;21:71–77.
42. Koss MJ, Hoffmann J, Nguyen N, et al. Proteomics of vitreous humor of patients with exudative age-related macular degeneration. *PLoS One*. 2014;9:e96895.
43. Schori C, Trachsel C, Grossmann J, Zygoula I, Barthelmes D, Grimm C. The proteomic landscape in the vitreous of patients with age-related and diabetic retinal disease. *Invest Ophthalmol Vis Sci*. 2018;59:AMD31–AMD40.
44. Banerjee S, Savant V, Scott RAH, Curnow SJ, Wallace GR, Murray PI. Multiplex bead analysis of vitreous humor of patients with vitreoretinal disorders. *Invest Ophthalmol Vis Sci*. 2007;48:2203–2207.
45. Ozawa GY, Bearse MA, Adams AJ. Male-female differences in diabetic retinopathy? *Curr Eye Res*. 2015;40:234–246.

Downloaded from abstracts.iovs.org on 04/19/2024